SEVERE THERMOREGULATORY DEFICIENCIES IN MICE WITH A GENE DELETION IN TITIN

By: Carissa Miyano

A Thesis

Submitted in Partial Fulfillment

of the Requirements for the Degree of

Master of Science

in Biology

Northern Arizona University

Spring 2018

Approved:

Kiisa Nishikawa, Ph.D., Chair

C. Loren Buck, Ph.D.

Tinna Traustadóttir, Ph.D.

ABSTRACT

SEVERE THERMOREGULATORY DEFICIENCIES IN MICE WITH A GENE DELETION IN TITIN

CARISSA A. MIYANO

Muscular dystrophy with myositis (*mdm*) mice, which carry a deletion in the muscle protein titin, shiver at a lower than expected frequency for their body size, have body temperatures that decrease below ambient temperatures of 34°C, and have reduced active muscle stiffness in vivo compared to their wild type siblings. The impairment in shivering thermogenesis could be due to the N2A deletion in the titin protein leading to more compliant muscles and lower shivering frequency. I hypothesized that the ability of *mdm* mice to use the other heat production mechanism, nonshivering thermogenesis (NST), may also be impaired and contribute to their hypothermic state. To assess the response to cold exposure, body temperature and metabolic rate were measured in wild type and *mdm* mice using open-flow respirometry at four ambient temperature ranges: 19-21°C, 23-25°C, 27-30°C, and 33-35°C. Following the temperature experiment, NST was maximally stimulated by administering 1.2 mg kg^{-1} of norepinephrine subcutaneously. In the temperature experiment, there was a significant interaction between genotype and temperature, with *mdm* mice having significantly higher metabolic rates at 27-30°C and lower metabolic rates at 23-25°C compared to wild type mice. After correcting metabolic rate for Q_{10} effects, *mdm* mice had lower metabolic rates compared to size-matched *Perognathus longimembris* (little pocket mouse). In addition, the capacity for NST, estimated by area underneath the metabolic response curve, was also reduced in *mdm* mice compared to wild type littermates. When comparing *mdm* mice to other mice with similar body mass (7g), the effects of low metabolic rate and capacity for NST were exacerbated because predicted values of metabolic rate and capacity for NST are larger for smaller animals. These results indicate that a deletion in N2A titin causes severe thermoregulatory defects at every level of thermoregulation, including NST. Direct effects of the titin mutation likely lead to the lower shivering frequency observed. Indirect effects likely lead to a lower capacity for NST and metabolism in general. Future studies should investigate effects on oxidative phosphorylation or other signaling pathways.

Acknowledgements

Many people have been crucial and supportive of this work both within NAU and outside of it. First, I must give thanks to my advisor, Dr. Kiisa Nishikawa. Her door was always open and she was supportive of career development both within and outside the Nishikawa lab. Kiisa emulates exactly what a strong leader should be and it has been a privilege to have an outstanding female scientist to look up to. Dr. Loren Buck challenged me to think deeper about my research and encouraged me to develop myself professionally outside of the lab. Without Loren, I would have never been pushed to attend a conference halfway across the world in Rio de Janeiro and meet world-renowned physiologists. Dr. Tinna Traustadóttir brought refreshing enthusiasm and an insightful point of view to my committee meetings. Tinna generously opened her lab to allow me to learn about the molecular side of my work and for that, I thank her and her students, Savannah Berry and Ethan Ostrom, for devoting time and patience to teaching me.

The Nishikawa Lab has supported me endlessly throughout my work. Uzma Tahir and Anthony Hessel are strong leaders that have given me countless hours of advice and moral support. Both their work in the Nishikawa lab and the Graduate Student Government show their passion for what they do. I want to thank the rest of the members of the Nishikawa Lab for not only providing support for this project but also making this lab a fun place to work and being the best softball team out there (go Titins!).

I want to thank Dr. Scott Nichols and Leslie Hempleman for their help with animal care, developing protocols, and assistance. I would also like to thank Danielle Dillon, who was always available to help me with my equipment. The NAU Statistical Consulting Lab, especially Dr. Roy St. Laurent, was also extremely helpful in helping me put together my statistical analysis for this project.

A special thanks goes out to my biology comrades here at NAU: Savannah Berry, Trevor Cotter, Ryan Moreno, and Victor Zhang. Thank you for supporting me and my work, whether it was listening to a presentation for the millionth time or showing me how to do calculus late at night. You have all made my life here in Flagstaff a wonderful experience.

My family has been on board and supportive of everything I have done here at NAU, even when I said "I'm going to Brazil in a month." Thank you for your continued support of my passion for physiology.

Finally, I would like to thank my sources of funding. The National Science Foundation (NSF IOS-0742483, NSF IOS-1025806, and NSF IOS-1456868), W.M. Keck Foundation, and the Technology Research Initiative Fund of Northern Arizona University provided support for this research. These grants and the NAU Department of Biology supported me as I completed this research. In addition, the NAU Graduate Student Government and the American Physiological Society provided funding for travel to conferences, where I had the privilege of presenting this work.

Contents

List of Figures

This thesis was written with the intent of submitting to the Journal of Experimental Biology.

Chapter 1: Introduction

Defense of a constant core body temperature (T_b) by generating or dissipating heat is one of the most important adaptations of homeothermic mammals to maintain homeostasis in hot or cold environments. This strategy allows small animals, which have a large surface area that readily loses heat to the environment, to survive and be active during times when other animals may be hibernating or inactive (Rowland et al., 2015). Large deviations in T_b can have severe consequences such as reduced enzyme efficiency, and altered diffusion capacity and membrane fluidity. These critical cellular functions can result in loss of consciousness, inability to coordinate and execute motor functions, and even death (Morrison & Nakamura, 2011). T_b is maintained during cold exposure by vasoconstriction of peripheral vessels, piloerection, postural changes, shivering thermogenesis, and nonshivering thermogenesis (Hemingway, 1963). A previous study found that mice with a mutation in the giant muscle protein titin cannot maintain T_b below 34°C and have a decreased tremor frequency during shivering thermogenesis (Taylor-Burt et al., 2015). In this study, we investigated the effect of the titin mutation on the other heat generating mechanism, nonshivering thermogenesis.

Nonshivering thermogenesis (NST) is a highly adaptive heat-generating mechanism that occurs through the uncoupling action of Uncoupling Protein-1 (UCP1) in brown adipose tissue of many animals, including rodents (Cannon & Nedergaard, 2004; Depocas, 1960; Golozoubova, 2006; Lowell et al., 1993; Meyer et al., 2010; Nedergaard et al., 2001; Nicholls & Locke, 1984). Like basal metabolic rate (BMR), the contribution of nonshivering thermogenesis to summit metabolism (VO_{2sum}) as well as VO_{2sum} itself, scales with body mass (Wunder & Gettinger, 1996). Thermogenic capacity, which can be approximated by VO_{2sum}, provides an estimate of an animal's ability to thermoregulate and refers to the total capacity for heat production during cold

exposure. Thermogenic capacity can be measured when both shivering thermogenesis (ST) and NST are maximally activated during acute cold exposure. The mouse, whose small body mass leads to increased levels of thermal conductance, has a higher contribution of NST to VO_{2sum} to offset heat loss in comparison to larger animals (Wunder & Gettinger, 1996).

The muscular dystrophy with myositis (*mdm*) mouse is characterized by a 779-bp deletion in the N2A region of the titin gene (Garvey et al., 2002) and a previous study demonstrated severe thermoregulatory deficiencies (Taylor-Burt et al., 2015). Mice homozygous for the *mdm* mutation have a severe and progressive degeneration of skeletal muscles and exhibit a lower body mass, stiffer gait, and reduced lifespan (Garvey et al., 2002; Huebsch et al., 2005; Lopez et al., 2008). Studies have demonstrated that *mdm* muscle has higher passive stiffness than wild type muscle (Hessel et al., 2017; Lopez et al., 2008; Monroy et al., 2017). In addition, Taylor-Burt et al. (2015) demonstrated *in vitro* that *mdm* mice have lower active muscle stiffness and a lower tremor frequency during ST, even after Q_{10} correction to account for temperature effects. It would be expected that mice with stiffer muscles would have increased tremor frequencies, therefore these results are consistent with the hypothesis that titin plays a key role in active muscle stiffness. The deficiency in shivering frequency likely led to the observed hypothermic state of *mdm* mice at temperatures below 34°C. The combination of increased thermal conductance and lower heat generation via ST results in an offset of heat production vs. heat loss, leading to severe thermoregulatory deficiencies in *mdm* mice. What is not known is whether the capacity for using the other heat generating mechanism, NST, is also impaired in *mdm* mice.

The purpose of this study was to investigate whether impairment of NST in *mdm* mice contributes to their observed hypothermia in addition to ST and thermal conductance. We tested

two hypotheses: 1) metabolic rates will reach a maximum at higher ambient temperatures (T_a's) than wild type mice due to the shifted thermoneutral zone (TNZ) of *mdm* mice; and 2) the inability to defend T_b cannot be explained solely by lower shivering frequencies, therefore an impairment in the other heat production mechanism, NST, is present.

Chapter 2: Materials and Methods

2.1 Mice

Animal experiments were approved by the Institutional Animal Care and Use Committee of Northern Arizona University. Breeding pairs of B6C3Fe *a-/a-mdm* mice (*Mus musculus* Linnaeus) from the Jackson Laboratory (Bar Harbor, ME, USA) were housed on a 14 h:10 h light:dark cycle at 23-24°C at Northern Arizona University. In this study, all animals were housed in an environmental chamber set to 34°C upon weaning and experiments were conducted during the dark phase of the light cycle when mice are active. Wild type mice were fed LabDiet 5001 Laboratory Rodent Diet and *mdm* mice were fed LabDiet 5LJ5 PicoLab High Energy Mouse Diet (LabDiet, St. Louis, Missouri, USA). *Mdm* mice were fed the high-fat-diet chow due to high mortality rates when fed standard laboratory chow. Wild type mice were housed singly or with siblings, if both were used in experiments. Each cage was equipped with bedding and enrichment.

Sample sizes for wild type and *mdm* mice were the following at four different temperatures unless otherwise noted: 19-21°C (n = 7 wild type, n = 5 *mdm*), 23-25°C (n = 6 wild type, n = 7 *mdm*), 27-30°C (n = 6 wild type, n = 8 *mdm*), and 33-35°C (n = 7 wild type, n = 8 *mdm*). Body mass differed significantly between genotypes (Welch's Test, $p < 0.001$) with *mdm* mice (n = 9, 7.2 ± 0.21g) being much smaller than wild type mice (n = 7, 26.0 ± 1.82g). For statistical analysis, body mass was normally distributed but variance of residuals was unequal between groups so a Welch's Test, whose means are weighted by the reciprocal of the group mean variances, was used to identify significant differences.

2.2 Study Design

In this study, mice underwent surgery followed by a one-week recovery period. The experimental period comprised of temperature experiments (Days 9-12) and norepinephrine (NE)-stimulated thermogenesis experiments (Figure 1).

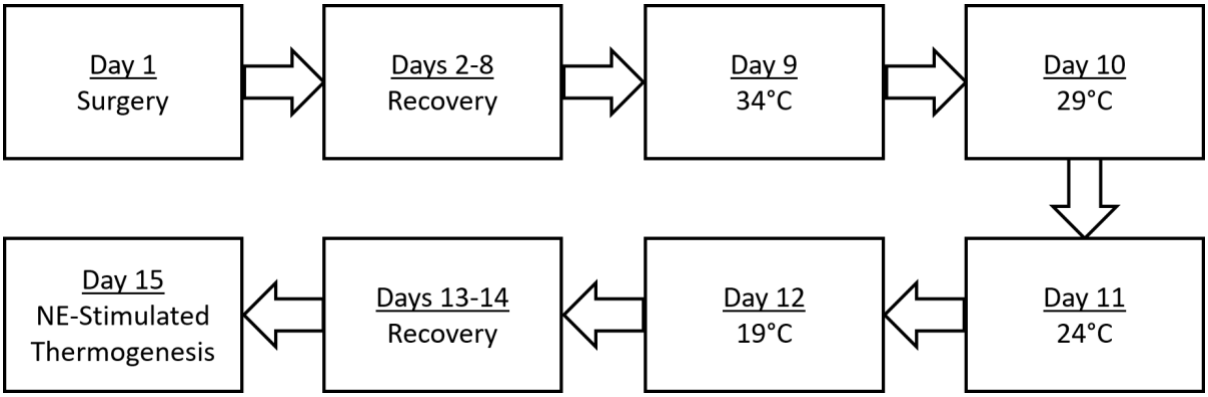

Figure 1: Study Design, including surgery, recovery, temperature experiments, and norepinephrine-stimulated thermogenesis.

2.3 Surgery

To measure core T_b, implantable recording devices were surgically placed in each mouse's peritoneal cavity at the age of 25-30 days old. Different temperature recording devices were used due to the smaller size of the *mdm* mice (7.23 ± 0.21g) compared to wild type siblings (25.97 ± 4.45g). For *mdm* mice, a Biothermo13 Passive Integrated Transponder (PIT) tag (0.109 ± 0.030g; Biomark, Boise, ID, USA) was surgically implanted in the peritoneal cavity. The transponder recorded T_b at a resolution of ± 0.5°C. Wild type mice were surgically implanted with a PhysioTel TA-F10 telemetry device (1.6g; Data Sciences International, St. Paul, MN, USA) which recorded T_b at a resolution of ± 0.05°C. During the surgery, mice were anesthetized with isoflurane USP (MWI Veterinary Supply, Boise, ID) using a Forane Vaporizer (Ohio Medical Corporation, Gurnee, IL, USA). Anesthesia was induced by placing the mouse in a

small chamber supplied with 1-2% isoflurane-oxygen mixture. Upon unconsciousness, the mouse was transferred to a heating pad where anesthesia was administered using a nosecone that delivered a 1-2% oxygen-isoflurane mixture. Once pedal reflex was absent, the abdominal fur was clipped and scrubbed with povidone iodine and 70% ethanol. The skin and muscle were incised and bluntly dissected to expose the peritoneal cavity. The device was then placed freely inside the peritoneal cavity and the muscle and skin were closed with 3-0 Maxon absorbable monofilament suture. Buprenorphine, an analgesic agent, was administered subcutaneously (0.10 mg kg^{-1}) for 72 hours following surgery. Post-surgery recovery lasted for 7 days at 34°C before further experiments were conducted.

2.4 Temperature Experiments

Mice were placed in 9L metabolic cages during the experiments. Oxygen consumption (VO_2) and carbon dioxide (CO_2) production measurements were obtained using a computer controlled open-flow respirometry system (Promethion, Sable Systems, Las Vegas, NV, USA). In this system, each cage had its own gas analysis chain for respiratory gases comprising a flow controller, capacitive water vapor partial pressure analyzer, spectrophotometric CO_2 analyzer, and fuel cell O_2 analyzer. Water vapor was continuously measured and its dilution effect on O_2 and CO_2 was compensated mathematically. The flow rate of each 9L cage was 2000 ml min^{-1} with a subsample rate of 250 ml min^{-1}, which allowed for approximately 12 complete air exchanges per hour. The gas analyzer was calibrated using 100% N_2 and a span gas with a known concentration of CO_2 mixed with N_2 prior to each set of experiments for an animal. The cages were housed inside an environmental chamber (Percival Scientific, Perry, IA, USA) so that T_a could be controlled and bedding was removed from each cage to prevent burrowing. Cages sat

on top of either an antennae reader or telemetry receiver (Biomark, Boise, ID, USA; Data Sciences International, St. Paul, MN, USA) to collect T_b data throughout the experiment. T_b was collected once per minute using either PhysioTel RPC-1 Receivers for the PhysioTel TA-F10 telemetry devices or HPR Plus PIT Tag Reader and Antennae for the BioTherm13 PIT tags (Data Sciences International, St. Paul, Minnesota, USA; Biomark, Boise, ID, USA). T_a was validated and recorded using a datalogger (Onset HOBO Data Logger, Bourne, MA, USA) with a resolution of ± 0.14°C.

VO_2 and CO_2 were collected once per second using SableScreen v3.3.11 acquisition software, with 60 samples averaged per minute for final analysis (Sable Systems International, Las Vegas, NV, USA). VO_2 (ml min^{-1}) was recalculated to milliliters of O_2 per gram of body mass per hour for each animal and is referred to hereafter as metabolic rate. Raw data was processed using ExpeData v1.8.4 (Sable Systems International, Las Vegas, NV, USA). For the temperature experiments, a subset of 10 minutes of continuous data was chosen for analysis that met the following requirements: 1) recordings occurred after the fasting period; 2) T_a did not exceed the specified temperature range for that experiment (19-21°C, 23-25°C, 27-30°C, 33-35°C); and 3) the 10 data points for oxygen consumption (ml O2 g^{-1} h^{-1}) were chosen when animal movement was minimal, which was measured by BXYZ-R beam arrays (Sable Systems, Las Vegas, NV). At the coldest temperatures (19-21°C and 23-25°C), wild type mice were more active than at the higher temperatures (27-30°C and 33-35°C), therefore the lowest activity points were chosen.

All mice underwent four 4-hour (*mdm)* or 5-hour (wild type) temperature experiments once per day for four consecutive days. To minimize the effect of diet-induced thermogenesis,

wild type mice were fasted for two hours at the onset of the experiment and *mdm* mice were fasted for only one hour due to their fragility. All mice were weighed before and after each experiment. For calculating mass-specific metabolic rate (ml O_2 g^{-1} h^{-1}), mass was assumed to be lost linearly during the experiment. The experimental temperatures (33-35°C, 27-30°C, 23-25°C, 19-21°C) were chosen based on a previous study which found that 34°C was the lower critical limit of the TNZ in *mdm* mice (Taylor-Burt et al., 2015). The 33-35°C temperature was used to establish resting metabolic rate for this study.

2.5 Q_{10} Effects on Metabolic Rate

Because *mdm* mice have low T_b below 34°C (Taylor-Burt et al., 2015), it is necessary to account for differences in metabolic rate that could be due to Q_{10} effects. Expected metabolic rate was calculated for *mdm* mice assuming a normal T_b of 37°C and a Q_{10} of 2.4 (Hudson and Scott, 1978) using the following equation:

$$MR_{expected} = MR_{observed} Q_{10}^{\frac{(37 - T_{observed})}{10}},$$

where $MR_{expected}$ is metabolic rate expected if T_b is 37°C, $MR_{observed}$ is observed metabolic rate and $T_{observed}$ is observed T_b. Once $MR_{expected}$ was calculated, it was subtracted from $MR_{observed}$ to estimate Q_{10} effects and is referred to hereafter as E-O Metabolic Rate.

2.6 Norepinephrine-Stimulated Thermogenesis

To compare the capacity for nonshivering thermogenesis between genotypes, a norepinephrine-stimulated thermogenesis experiment was conducted using wild type (n = 6) and *mdm* mice (n = 6). Similar to the temperature experiment, mice were fasted for either 1 or 2 hours (*mdm* and wild type, respectively; Speakman, 2013) to avoid diet-induced thermogenesis.

Experiments were conducted at 33-35°C to ensure that metabolic rate increase for all mice was not due to shivering thermogenesis (Van Sant & Hammond, 2008). At the start of the experiment and following the fasting period, mice were briefly removed from the metabolic cages to administer 1.2 mg kg^{-1} of norepinephrine (Wunder & Gettinger, 1996) subcutaneously and recordings were taken for the remaining 2-3 hours of the experiment. Subsequent rise in metabolic rate after injection yielded a metabolic curve from which thermogenic capacity due to nonshivering thermogenesis was calculated by taking the integral of the increase in metabolic rate after norepinephrine injection, computed numerically using the Trapezoidal Rule. A baseline metabolic rate was calculated as the average of 10 recordings before the animal was removed from the cage and injected with norepinephrine. This was subtracted from the calculation to account for animals that had higher or lower VO_2 before injection. The area calculation began with the onset of injection and ended when VO_2 reached previously calculated baseline values. The duration of the metabolic curve, referred to as total effect time, as well as time to peak metabolic rate and peak metabolic rate were measured test for differences in norepinephrine response between genotypes. In addition, peak T_b and average T_b were compared between genotypes after norepinephrine injection to test whether T_b followed the same trend as metabolic rate. Peak T_b was defined as the highest 60 s average and average T_b was the average T_b during the test.

2.7 Thermogenic Capacity

Thermogenic capacity can be approximated by VO_2 sum (Wunder & Gettinger,1996) as:

$$VO_2sum = BMR + ST + NST,$$

where VO_2sum is summit metabolism, BMR is basal metabolic rate, ST is shivering thermogenesis, and NST is nonshivering thermogenesis. VO_{2sum} will be referred to hereafter as thermogenic capacity. Relative contributions of ST, NST, and BMR to thermogenic capacity were calculated by rearranging the above equation. Metabolic rate during 33-35°C was used for calculations of BMR. To calculate NST, BMR was subtracted from peak metabolic rate during norepinephrine-stimulated thermogenesis (n = 6 wild type, n = 6 *mdm*) to parse out metabolic rate due solely to NST. Because the mice were not in a completely post-absorptive state during either experiment, NST was likely underestimated. Taylor-Burt et al. (2015) previously reported thermogenic capacity, therefore ST was calculated by subtracting peak metabolic rate during norepinephrine-stimulated thermogenesis (BMR + NST) from thermogenic capacity.

2.8 Statistical Analysis

Statistical analysis was performed using JMP v12 (SAS Institute, Inc., Cary, NC, USA). Values are reported as mean ± SEM and an alpha level of 0.05 was used for all tests.

Throughout the study, the *mdm* group at 19-21°C had a large within-group variance, leading to unequal variances when comparing against wild type mice. Therefore, data was ranked using temperature as a blocking variable (19-21°C, 23-25°C, 27-30°C, 33-35°C). A Mixed Model ANOVA with subject nested within genotype and fixed effects of temperature and genotype was conducted for T_b, metabolic rate, and Q_{10} effects data. Steel-Dwass Multiple Comparisons were used to identify significant differences between genotypes at all temperatures. For the NE-stimulated thermogenesis data, Welch's test for unequal variances was used to identify significant differences in peak T_b, average T_b, and time to peak. T tests were used for peak metabolic rate, total effect time, and NST capacity. To identify significant differences in

absolute contributions to thermogenic capacity, t tests were used to compare ST and NST between genotypes.

Chapter 3: Results

3.1 Body Temperature

Mdm mice exhibit hypothermic characteristics as shown by their lower T_b's in comparison to wild type mice at lower T_a's. There was a significant effect of genotype and temperature on T_b (Mixed Model ANOVA on Ranks, $p < 0.001$) but no interaction between temperature and genotype. I found a significant effect of subject ($p < 0.05$). Post-hoc tests revealed significant differences between genotypes at all temperatures (Steel-Dwass, $p < 0.05$; **Figure 2**). At 19-21°C, 23-25°C, 27-30°C, and 33-35°C, I observed the following differences in T_b between wild type and *mdm* mice, respectively: 8.8°C, 4.2°C, 1.9°C, and 1.4°C.

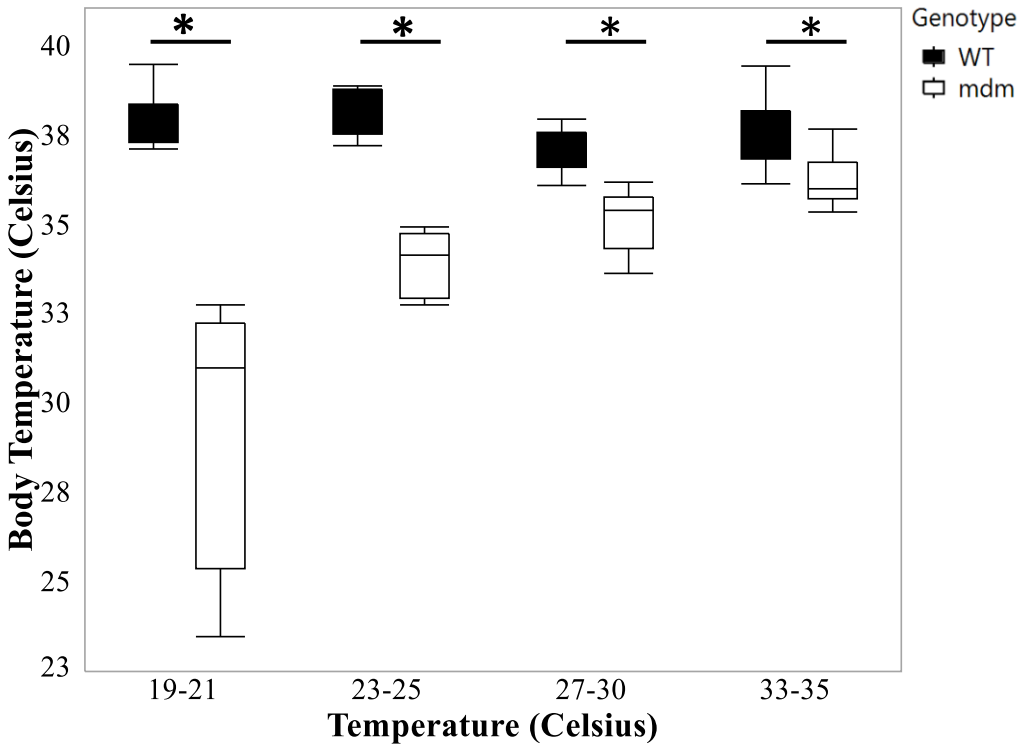

Figure 2: The relationship between T_b and T_a in wild type and *mdm* mice. Temperatures used were within a range of T_a's beginning at the thermoneutral zone of *mdm* mice (Taylor-Burt et al. 2015) and ending at lower T_a's in order to observe how well T_b could be defended ($p < 0.05$*).

3.2 Metabolic Rate

At 23-25°C, *mdm* mice begin to fail to thermoregulate, as demonstrated by significantly lower metabolic rates (**Figure 3**) and T_b's in comparison to wild type mice (**Figure 2**). In addition, *mdm* mice activate shivering and nonshivering thermogenesis more than wild type mice at 27-30°C, as demonstrated by their higher metabolic rate. Despite their higher metabolic rate, their T_b remains lower than that of wild type mice.

There was a significant interaction between genotype and temperature on metabolic rate (Mixed Model ANOVA on Ranks, $p < 0.05$). Wild type and *mdm* mice did not differ significantly at 33-35°C ($p > 0.05$, Steel-Dwass Multiple Comparisons). At 27-30°C, the metabolic rate of *mdm* mice (2.4 ± 0.12 ml O_2 g^{-1} h^1) was significantly than wild type mice (1.9 ± 0.09 ml O_2 g^{-1} h^{-1}; Steel-Dwass Multiple Comparisons, $p < 0.05$). At 23-25°C, metabolic rates for wild type mice (3.9 ± 0.19 ml O_2 g^{-1} h^{-1}) were significantly higher than *mdm* mice (3.1 ± 0.34 ml O_2 g^{-1} h^{-1}). Wild type mice (4.8 ± 0.29 ml O_2 g^{-1} h^{-1}) were not significantly different from *mdm* mice (3.5 ± 0.68 ml O_2 g^{-1} h^{-1}) at 19-21°C (Steel-Dwass Multiple Comparisons, $p = 0.1939$). This was likely due to the large variability at 19-21°C compared to wild type mice (**Figure 4**). Data points that were 1.5 times the interquartile range were excluded from the final analysis, one of which was an *mdm* outlier in the 23-25°C range.

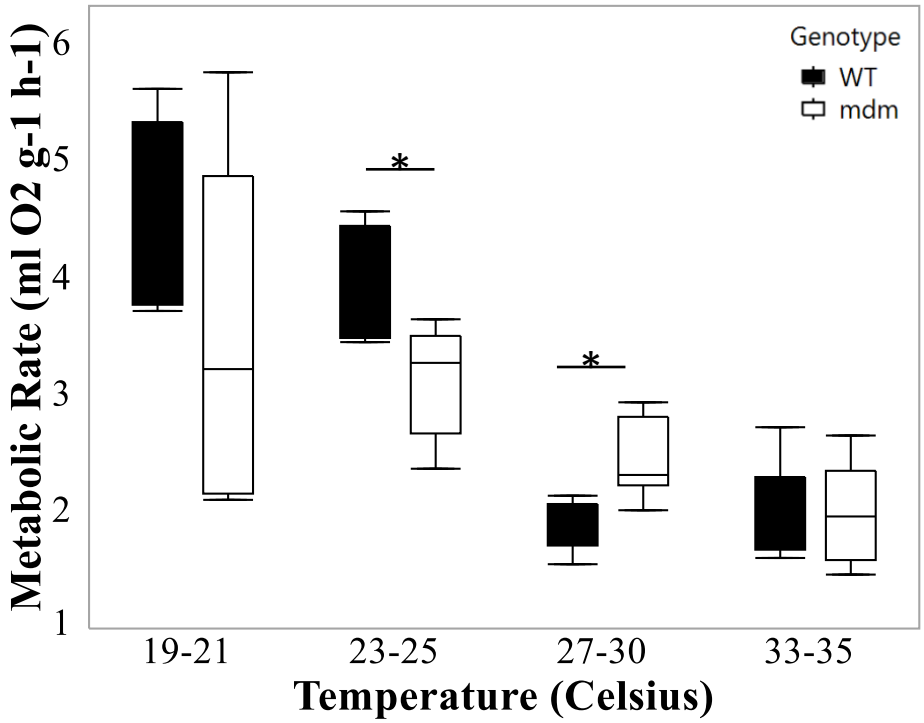

Figure 3: The relationship between metabolic rate and ambient temperature. Temperatures used were within a range starting at the thermoneutral zone for *mdm* mice, where metabolic rate was expected to be at resting levels, to lower T_a's at which metabolic rate was expected to increase ($p < 0.05$*).

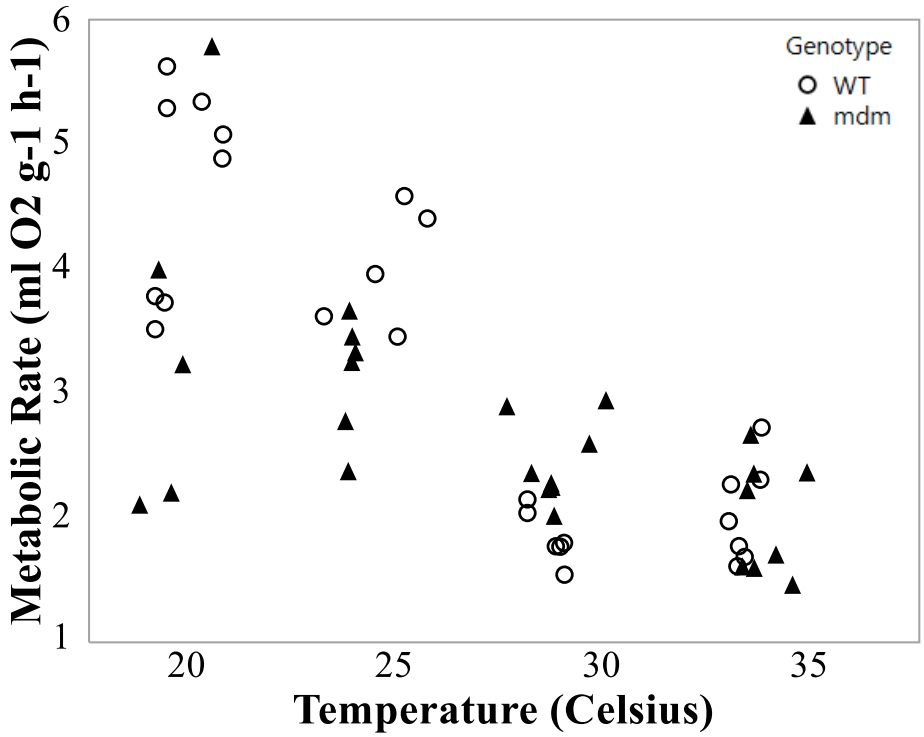

Figure 4: Individual metabolic rate measurements highlight variability of *mdm* mice at colder temperatures. Points represent individuals and shapes represent genotypes.

3.3 Q_{10} Effects on Metabolic Rate

In general, *mdm* mice had $MR_{observed}$ values far lower than $MR_{expected}$ values, with the largest differences in E-O at the lower temperatures (**Figure 5**). Wild type mice tended to remain close to $MR_{expected}$, except at lower temperatures where $MR_{observed}$ was higher than predicted. The higher E-O values for wild type mice at lower temperatures are likely due to certain subject's having higher activity thus subsequent metabolic rate at lower temperatures (observational).

A significant effect of genotype was found on E-O metabolic rate (Mixed Model ANOVA on Ranks, $p < 0.001$) and *mdm* mice had significantly higher E-O in comparison to wild type mice at all temperatures. The largest differences in E-O were seen at the two lowest temperatures. At 23-25°C, *mdm* mice (1.0 ± 0.08 ml O_2 g^{-1} h^{-1}) had significantly higher E-O in comparison to wild type mice (-0.4 ± 0.10 ml O_2 g^{-1} h^{-1}) who had higher observed values than predicted, making their E-O negative (Steel-Dwass Multiple Comparisons, $p < 0.05$). At the lowest temperature of 19-21°C, *mdm* mice (3.0 ± 0.46 ml O_2 g^{-1} h^{-1}) fell short of their expected metabolic rate in comparison to wild type mice (0.4 ± 0.32 ml O_2 g^{-1} h^{-1}) who had higher observed values (Steel-Dwass Multiple Comparisons, $p < 0.05$).

Surprisingly, *mdm* mice $MR_{expected}$ fell short of predicted metabolic rates for the size matched *Perognathus longimembris* at the selected temperature ranges. Allometric relations of metabolic rate with T_a have been reported for the 8.2g *Perognathus longimembris* (little pocket mouse; Chew et al., 1967). Therefore, the average temperature of each of the T_a ranges was used to predict metabolic rates of the little pocket mouse (Figure 6). For each of the temperature ranges (19-21°C, 23-25°C, 27-30°C, 33-35°C), differences in $MR_{expected}$ between the little pocket mouse and *mdm* mice were as follows: 0.54 ml O_2 g^{-1} h^{-1}, 1.69 ml O_2 g^{-1} h^{-1}, 1.65 ml O_2 g^{-1} h^{-1}, and 0.85 ml O_2 g^{-1} h^{-1}.

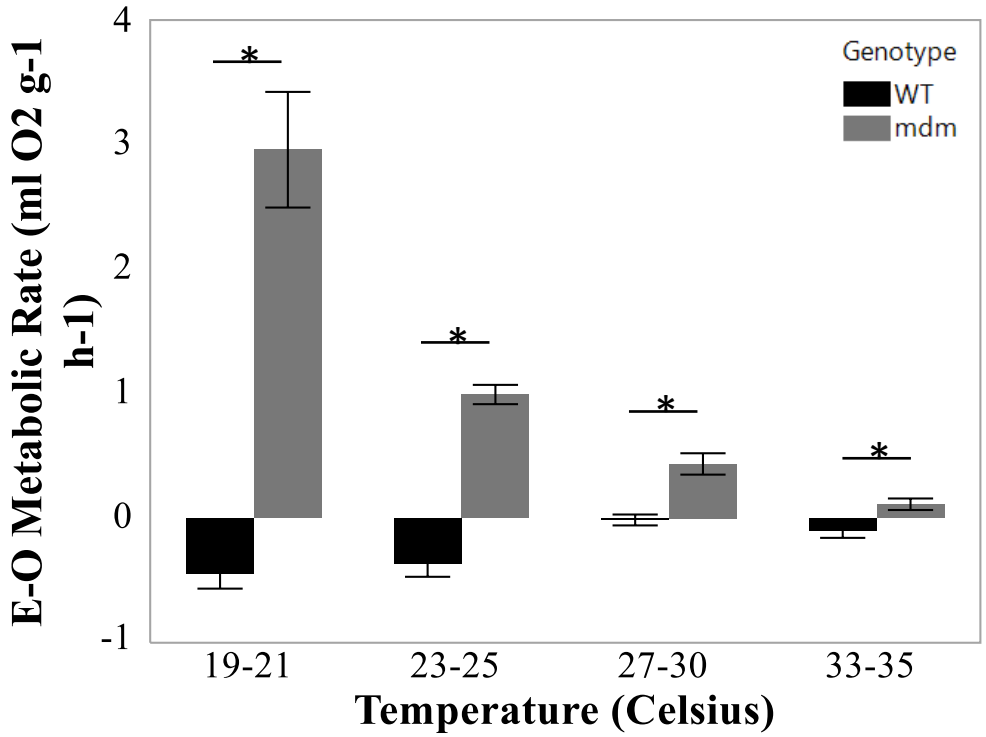

Figure 5: The relationship between expected-observed (E-O) metabolic rate and ambient temperature. The Q_{10} equation was rearranged to find $MR_{expected}$ if mice had T_b's of 37°C and a Q_{10} of 2.4 (Hudson and Scott 1978) and it was compared with $MR_{observed}$ to investigate T_b effects on metabolic rate between genotypes ($p < 0.05$*).

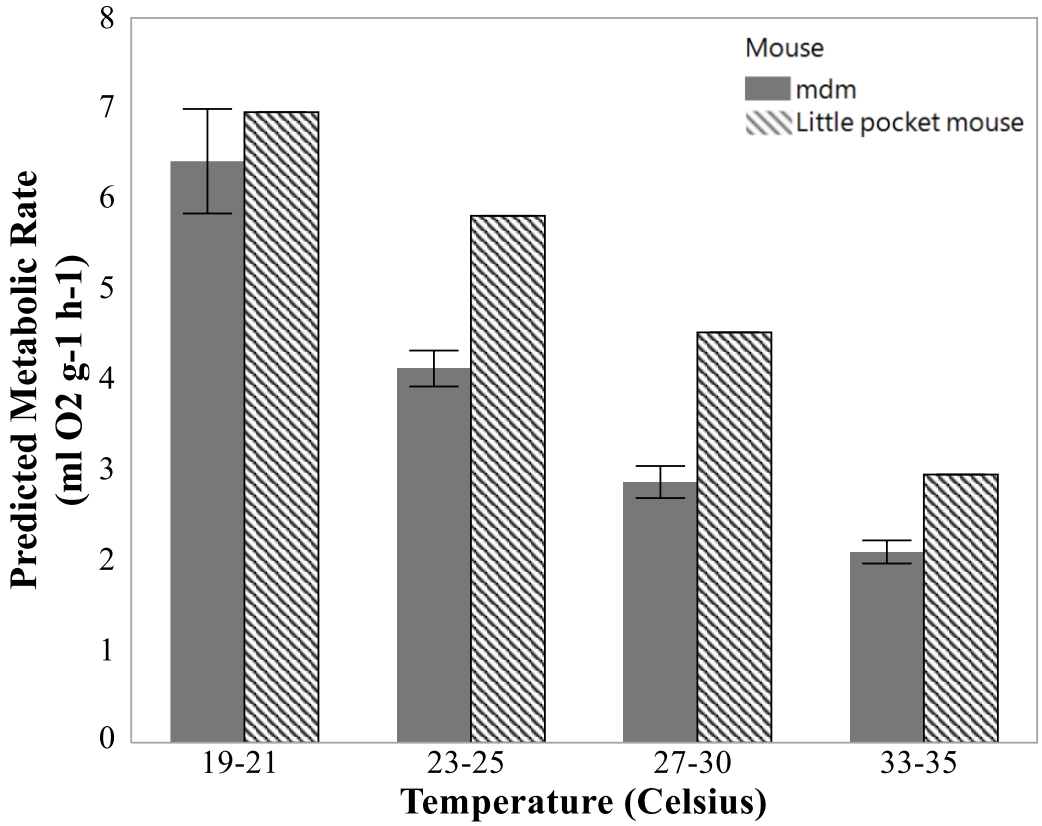

Figure 6: Comparison of $MR_{expected}$ between *mdm* and *Perognathus longimembris* (little pocket mouse). Due to the small size of *mdm* mice (7.23 ± 0.21g), $MR_{expected}$ was compared to the size-matched little pocket mouse (8.2g; Chew et al., 1967) at the mean value of the T_a ranges.

3.4 Norepinephrine-Stimulated Thermogenesis

After norepinephrine injection, wild type mice (143.9 ± 20.01 ml O2 g^{-1} h^{-1}) had a significantly higher capacity for nonshivering thermogenesis than *mdm* mice (62.3 ± 22.78 ml O_2 g^{-1} h^{-1}; t test, $p < 0.05$). There was no significant difference between genotypes in the time to reach peak metabolic rate (Welch's Test, $p = 0.60$) or the total effect time (t test, $p = 0.08$; **Figure 7**). Wild type mice took 17.3 ± 2.20 minutes to reach peak metabolic rate and *mdm* mice took 22.8 ± 9.65 minutes. Total effect time for wild type and *mdm* mice was 66.3 ± 4.92 minutes and 48.3 ± 10.44 minutes, respectively.

Both wild type and *mdm* mice exhibited similar metabolic profiles following norepinephrine injection, but had significantly different peak T_b and average T_b (**Figure 8**). Interestingly, genotypes did not differ in peak metabolic rate reached after injection (t test, $p = 0.21$) with wild type mice reaching 7.2 ml O_2 g^{-1} h^{-1} and *mdm* mice reaching 6.4 ml O_2 g^{-1} h^{-1}. However, wild type mice (39.7 ± 0.08 ℃) reached a higher peak T_b (Welch's Test, $p < 0.05$) than *mdm* mice (38.5 ± 0.35 ℃) during the trial. In addition, wild type mice had a significantly higher average T_b (38.7 ± 0.24 ℃) in comparison to *mdm* mice (37.3 ± 0.33 ℃; Welch's Test, $p < 0.05$).

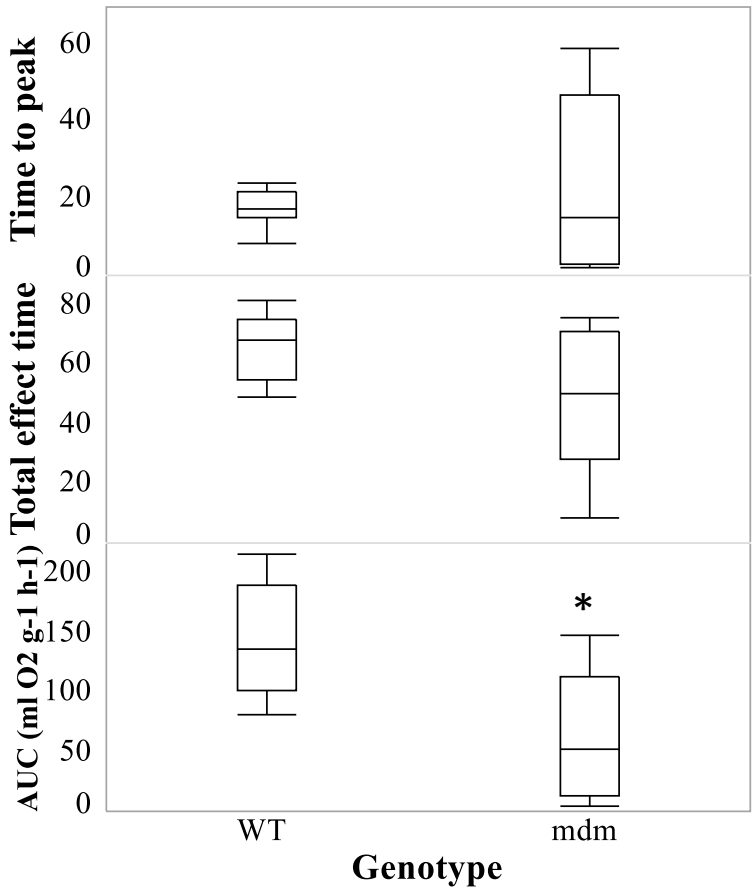

Figure 7: Time to reach peak metabolic rate, total effect time, and area under the curve between genotypes after norepinephrine injection. *Mdm* mice had a smaller area underneath the metabolic curve, therefore a lower capacity for nonshivering thermogenesis after norepinephrine injection (1.2 mg^{-1} kg^{-1}) in comparison to wild type mice (n = 6 wild type, n = 6 *mdm;* $p < 0.05$*). The amount of time it took to reach peak metabolic rate was not significant between groups ($p = 0.60$) nor was the total effect time of norepinephrine on metabolic rate ($p = 0.08$).

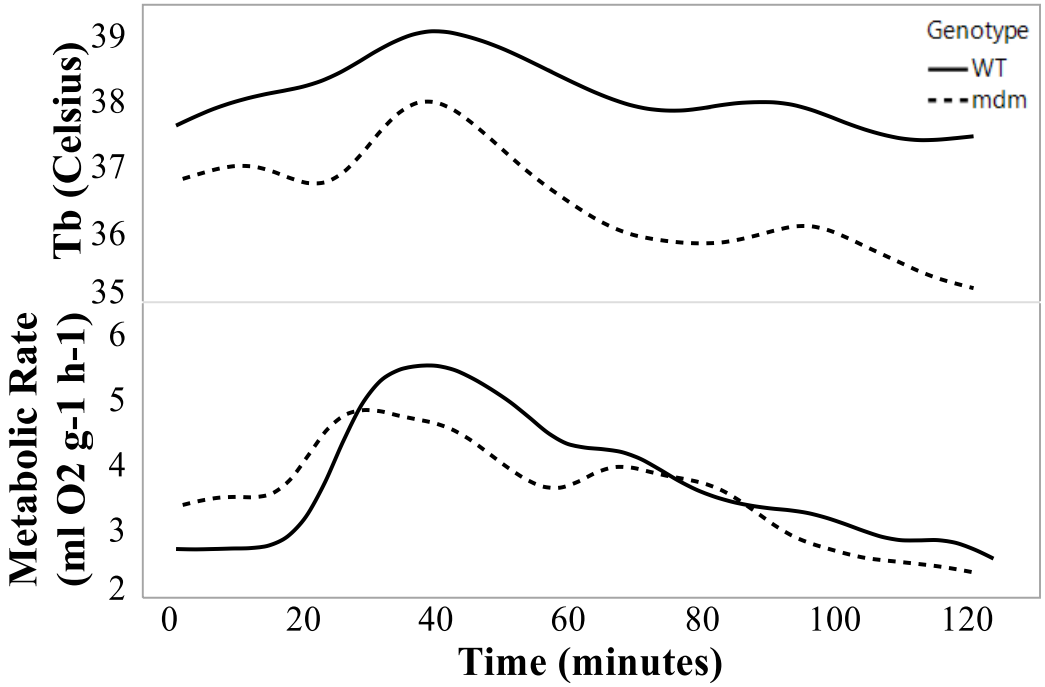

Figure 8: T_b and metabolic rate responses to norepinephrine in wild type and *mdm* mice. Wild type mice had significantly higher peak T_b and average T_b in comparison to *mdm* mice (n = 6 wild type, n = 6 *mdm*; Welch's Test, $p < 0.05$). Genotypes did not differ in peak metabolic rates (t test, $p = 0.11$).

3.5 Contributions to Thermogenic Capacity

There was no difference between wild type and *mdm* mice in the contributions of BMR, ST, and NST to thermogenic capacity (Figure 9). Taylor-Burt et al. (2015) reported thermogenic capacity to be 11.1 ml O_2 g^{-1} h^{-1} and 10.4 ml O_2 g^{-1} h^{-1} for wild type and *mdm* mice respectively. As previously reported, metabolic rates recorded during the 33-35°C temperature range were not significantly different between genotypes, which was used as BMR for calculations of thermogenic capacity. ST accounted for 3.9 ± 0.17 ml O_2 g^{-1} h^{-1} of wild type thermogenic capacity and 3.9 ± 0.86 ml O_2 g^{-1} h^{-1} of *mdm* thermogenic capacity (t test, $p = 0.95$). In addition, there were no differences in NST contributions to thermogenic capacity for wild type (5.7 ± 0.17 ml O_2 g^{-1} h^{-1}) and *mdm* mice (4.9 ± 0.86 ml O_2 g^{-1} h^{-1}; t test, $p = 0.42$).

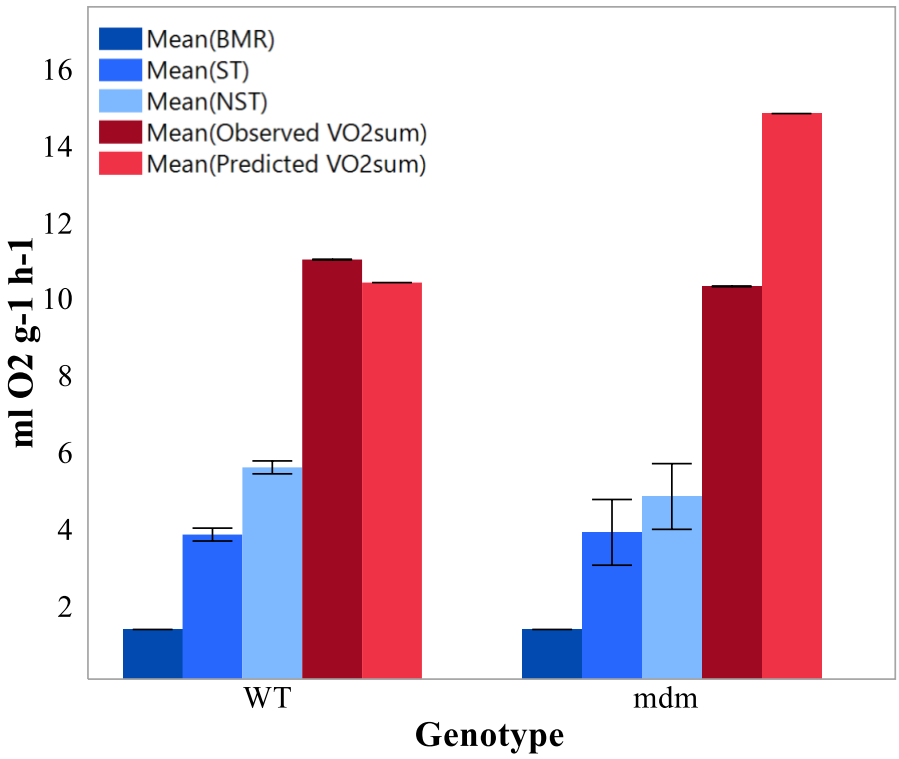

Figure 9: Contributions of BMR, ST, and NST to thermogenic capacity (VO_{2sum}) and predicted thermogenic capacity (VO_{2sum}) in wild type and *mdm* mice. Wild type and *mdm* mice did not differ significantly in the contributions of BMR ($p > 0.05$), ST ($p = 0.53$), and NST ($p = 0.21$) to thermogenic capacity ($n = 6$ wild type, $n = 6$ *mdm*; t tests). *Mdm* mice observed thermogenic capacity from Taylor-Burt et al.'s (2015) study fell short of predicted thermogenic capacity based on body size.

Chapter 4: Discussion

In this study, I examined the capacity for nonshivering thermogenesis in *mdm* mice to investigate whether this component of heat production at the brown adipose tissue level is impaired, in addition to the heat production mechanism at the muscular level, shivering thermogenesis (Taylor-Burt et al., 2015). I confirmed the inability of *mdm* mice to maintain homeothermy by measuring their T_b and metabolic rate across a range of T_a's. *Mdm* mice had lower T_b's at all T_a's and lower metabolic rates at 23-25°C, compared to wild type mice.

Because *mdm* mice could not defend their core T_b, I observed significant Q_{10} effects on metabolic rate. E-O metabolic rate was significantly higher for *mdm* mice indicating that even if *mdm* mice could maintain normal T_b's, they would not be able to generate a normal metabolic rate. Therefore, size comparisons were necessary. Surprisingly, I found that predicted metabolic rates of *mdm* mice fell short of the size-matched little pocket mouse. I also found that the capacity for nonshivering thermogenesis is significantly lower in *mdm* mice compared to wild type mice, indicating that this component of heat generation is also impaired. The relative contributions of basal metabolic rate, shivering thermogenesis, or nonshivering thermogenesis to VO_{2sum} did not differ between wild type and *mdm* mice. My results demonstrate that a gene deletion in titin not only results in a deficiency in shivering thermogenesis, but it impacts nonshivering thermogenesis as well, likely contributing to lower T_b, metabolic rate, and thermogenic capacity.

4.1 Body Temperature

Mdm mice had significantly lower T_b's than wild type mice, even at 33-35°C, indicating that this temperature range is near the lower critical limit of the TNZ (**Figure 2**). My findings

suggest that in order for *mdm* mice to have euthermic T_b's similar to wild type mice, T_a needs to be even higher than 34-35°C, as previously reported by Taylor-Burt et al. (2015).

A reduction in T_b set point due to torpor, a behavioral thermoregulation strategy used by certain endotherms, is unlikely due to the pattern of metabolic rate and T_b observed. Torpor is induced by low T_a and/or depletion of metabolic fuels and is characterized by a reduction in T_b set point that leads to a precipitous decline in T_b, followed by a drop in metabolic rate (Geiser et al., 2014). During hypothermia, however, T_b set point is at euthermic levels, therefore T_b and metabolic rate drop slowly at first as thermoregulation fails and then decline rapidly once the body begins to cool. *Mdm* mice did not exhibit rapid declines in T_b followed by metabolic rate. Instead, I observed increases in metabolic rate upon cold exposure followed by a gradual reduction, indicating that *mdm* mice are attempting to thermoregulate but fail to keep T_b at euthermic levels. In addition, Hudson and Scott (1978) measured T_b and metabolic rate in *Mus musculus* and found that torpid mice with T_b's of 32°C had metabolism 50% of what was observed at euthermic T_b levels. The mice in this study had similar T_b values of 29.3 ± 1.7 °C at 19-21°C but had higher metabolic rates of 3.5 ± 0.68 ml O_2 g^{-1} h^{-1} in comparison to metabolic rates of 2.0 ± 0.16 ml O_2 g^{-1} h^{-1} at 33-35°C. These results support the conclusions that *mdm* mice fail to thermoregulate at cold temperatures and do not adopt the behavioral strategy of hypometabolism through torpor.

Studies have shown thermoregulatory deficiencies specific to nonshivering thermogenesis in UCP1-null mice, mice with induced obesity and Type II diabetes due to leptin alterations (*ob/ob* and *db/db*), and mice with inherited effects of fatty acid oxidation. UCP1-null mice were able to acclimate and tolerate 18°C with a well-defended T_b that was not significantly different from wild type mice (Golozoubova, 2006). However, adaptive nonshivering

thermogenesis was significantly altered in UCP1-null mice, which is discussed in further detail later. Mice with induced rapid early-onset obesity and diabetes, termed *ob/ob* and *db/db,* have marked reductions in nonshivering thermogenesis (Yen, et al., 1974). T_b of *ob/ob* and *db/db* mice were 30 ± 1.4 °C and 26.8 ± 8 °C after 90 minutes of exposure to 4°C. This is comparable to *mdm* mice at 19-21°C with T_b values of 29.3 ± 1.2 °C. In addition, mice homozygous for the inactivated allele BALB/cByJ, which encodes the short chain acyl CoA dehydrogenase, have abnormal nonshivering thermogenesis (Guerra et al., 1998). In BALB/cByJ mice, T_b dropped 10°C in less than 4 h at 4°C, which is similar to *mdm* mice at 19-21°C.

The impact of shivering thermogenesis on maintenance of T_b can be assessed by blocking muscular activity via curare-like drugs, which competitively block the binding of acetylcholine to the motor endplates of striated muscles (Bowman, 2006; Kashimura et al., 1992). In a study that blocked 50% of shivering via curare, wild type mice were still able to maintain a T_b of 35.4 ± 0.4 °C at 4°C (Bal et al., 2012), likely due to their ability to compensate via nonshivering thermogenesis and skeletal-muscle based thermogenesis. It is difficult to compare thermoregulatory deficits of *mdm* mice to genetically altered mice in other studies due to 4°C being the standard cold temperature versus 19-21°C, which was used in this study. Nonetheless, the *mdm* mice in this study have more severe thermoregulatory defects than mice with deficits in either shivering or nonshivering thermogenesis discussed above. This is likely due to the combined defects of both shivering and nonshiverering thermogenesis in *mdm* mice.

4.2 Metabolic Rate

Mdm and wild type mice maintained similar resting metabolic rates at temperatures of 33-35°C (2.0 ± 0.15 ml O_2 g^{-1} h^{-1} for wild type and *mdm* mice; **Figure 3**). These values are

comparable to resting metabolic rates reported for *Mus musculus* that were fasted between 5 and 30h and had metabolic rates of 1.47 ml O_2 g^{-1} h^{-1} (Hudson and Scott, 1978). The mice in this study were fasted for only 2 (wild type) or 1 (*mdm*) hour(s) which could account for the slightly higher metabolic rates found in this study.

Mdm mice fail to thermoregulate at temperatures below 27-30°C and are more cold-stressed than wild type mice at this temperature. This is demonstrated by their significantly higher metabolic rates compared to wild type mice (**Figure 3**). Wild type mice had comparable metabolic rates at 33-35°C and 27-30°C likely because these temperatures are near the TNZ (31-35°C ; Hudson and Scott, 1978). It is interesting that although *mdm* mice have higher metabolic rates than wild type mice at 27-30°C, there was still a significant difference in T_b, with *mdm* mice having lower T_b's than wild type mice. These results indicate that at this temperature, *mdm* mice work harder than wild type mice to thermoregulate as evidenced by higher metabolic rates, yet they still cannot maintain as high of a T_b as wild type mice. The failure to maintain a higher T_b despite higher metabolic rates is likely due to increased thermal conductance of *mdm* mice.

At 23-25°C, there was a large difference in metabolic rate between *mdm* and wild type mice, with wild type mice having significantly higher metabolic rates (**Figure 3**). There were no significant differences in metabolic rates between wild type and *mdm* mice at 19-21°C, which was interesting considering T_b differences were even more drastic between genotypes. This is likely due to the large standard error in metabolic rate observed with the *mdm* mice at this temperature in comparison to wild type mice.

Large differences in E-O metabolic rate combined with the little pocket mouse data demonstrated that even if *mdm* mice could properly defend T_b, normal metabolic rates could not be attained (**Figure 5**). Wild type and *mdm* mice differed significantly at all temperatures for E-

O metabolic rate. In general, wild type mice had $MR_{expected}$ values close to $MR_{observed}$ leading us to conclude that they had Q_{10} values near 2.4, which is typical of *Mus musculus* that are euthermic (Hudson & Scott, 1978). This was also demonstrated by the T_b data (Figure **2**). *Mdm* mice, in contrast, had much higher $MR_{expected}$ than $MR_{observed,}$ leading to high E-O metabolic rate. Metabolic rates of a similarly sized mouse, *Perognathus longimembris* (little pocket mouse), have reported regression values during varying T_a's (Chew et al., 1976) which was used to compare due to body mass allometrically scaling with metabolic rate (Kleiber, 1932). *Mdm* mice still fall short in metabolic rate even after correcting for Q_{10} effects in comparison to little pocket mice, especially at 23-25°C and 27-30°C with differences of 1.7 ml O_2 g^{-1} h^{-1} and 1.8 ml O_2 g^{-1} h^{-1}, respectively. Q_{10} effects exacerbate but do not completely account for lower metabolic rates in *mdm* mice even after considering their much smaller size in comparison to wild type mice.

4.3 Nonshivering Thermogenesis

Maximal VO_2 response to NE correlates well with body mass and is affected by acclimation temperature, with cold acclimated animals having higher VO_2 responses. Allometric relations for maximal metabolic response to norepinephrine in small mammals has been described by Wunder & Gettinger (1996) and includes a BMR component that can be used for animals acclimated to 23°C. Using this equation, the VO_2 response of wild type and *mdm* mice to NE was predicted to be 6 ml O_2 g^{-1} h^{-1} and 11 ml O_2 g^{-1} h^{-1}, respectively. Observed maximal VO_2 responses to NE values for wild type and *mdm* mice were 7.2 ml O_2 g^{-1} $h^{-1}$and 6.4 ml O_2 g^{-1} h^{-1}, which were not significantly different from one another. The animals in this study were housed at approximately 33-35°C from the time of surgery to the experiment (approximately 2 weeks), which could lead to smaller VO_2 responses in comparison to expected responses based on

Wunder and Gettinger's (1996) equation. Instead, wild type mice had slightly higher than expected VO_2 responses and *mdm* mice fell short of expected responses. *Mdm* mice were euthermic for these measurements since they were conducted at 33-35°C (Figure 2), therefore, Q_{10} effects cannot explain their smaller response to NE. These comparisons provide further evidence that *mdm* mice have a lower VO_2 response to NE than wild type mice.

Although *mdm* mice have a lower capacity for nonshivering thermogenesis, their responses (**Figure 7**) for time to peak metabolic rate, total effect time of NE, and peak metabolic rate were similar to those of wild type mice. Peak T_b and average T_b were significantly higher in wild type mice after norepinephrine injection in comparison to *mdm* mice (**Figure 8**). These results are consistent with the result that *mdm* mice have a reduced capacity for nonshivering thermogenesis, and therefore are unable to produce as much heat as wild type mice. Similarly, they were unable to maintain a high T_b for the total trial time as evidenced by significantly lower average T_b. This could have been due to their increased thermal conductance or to a depletion of metabolic fuels needed for nonshivering thermogenesis, primarily free fatty acids and glucose (Townsend & Tseng, 2014).

It is unlikely that the lower capacity of nonshivering thermogenesis in *mdm* mice can be explained by complete UCP1 absence. In wild type and UCP1-null mice that were warm-acclimated to 30°C, norepinephrine evoked large increases in metabolic rate for wild type mice and small increases for UCP1-null mice (Golozoubova, 2006). The small increase seen in UCP1-null mice was attributed to either UCP1-independent adrenergic thermogenesis or a general activation of adrenergic receptors. The mice in this study did not have significantly different peak VO_2 response to NE compared to wild type mice (**Figure 8**), therefore, a solely adrenergic effect causing metabolic rate increase in *mdm* is not likely. An interesting line of thought is the

possibility for decreased UCP1 expression or decreased sensitivity in brown adipose tissue to NE in *mdm* mice.

Mdm mice are impacted at the brown adipose tissue level and it is unlikely they are affected at the sympathetic outflow level. The nonshivering thermogenesis response was measured directly from UCP1 in brown adipose tissue by mimicking a maximal sympathetic response through administration of NE. Therefore, *mdm* mice are impacted significantly at this level. However, sympathetic outflow from neural outputs are also of interest during normal cooling-evoked thermogenesis. High-fat diet (HFD) has been shown to significantly reduce the cold-induced increase in BAT sympathetic nerve activity (SNA) and BAT thermogenesis via a vagal afferent mechanism in rats maintained on a HFD for ≥ 60 days (Madden & Morrison, 2016) as well as basal sympathetic activation of BAT in rats after 3, 6, and 9 weeks of HFD (Sakaguchi et al., 1989). The *mdm* mice in this study were fed HFD due to high morbidity rates associated with maintaining them on normal chow diets and they still exhibited emaciated appearances (Taylor-Burt et al., 2015) instead of obese phenotypes typical of animals fed HFD. While I cannot rule out HFD-induced dysfunction in sympathetic outflow as a contributor to decreased NST capacity, I would expect to see larger deficits in NST capacity in the *mdm* mice due to combined effects.

Titin has been implicated as a regulator in mitochondrial respiration as well as bioenergetics. The *sallimus* (*sls*) gene in drosophila, whose product is homologous to the NH2-terminal half of titin in vertebrates, has been identified as a transcription regulator of mitochondrial respiration (Jumbo-Lucioni et al., 2012). Jumbo-Lucioni et al. (2012) observed the natural variation between state 3 and state 4 mitochondrial respiration and found a direct effect of *sls* on mitochondrial function. Homozygous sls^{d00134} flies, which have a missing allele from

the *sls* gene, had 17% lower mitochondrial state 3 and 18% higher state 4 rates than controls. These results reveal that *sls* is a novel gene hub for regulation of mitochondrial respiration and that specific alleles of this gene can control naturally occurring variation in mitochondrial function. In addition, truncating titin variants (TTNtv) that cause genetic dilated cardiomyopathy (DCM) have been shown to alter mitochondrial bioenergetics (Verdonschot et al., 2018). In patients with TTNtv, increased expression of genes across all electron transport chain complexes as well as ATP synthase was found. These findings suggest a compensatory response of increased oxidative phosphorylation components in order to counteract limited contractile ability of cardiac tissue as an indirect effect of a titin mutation.

Defects in oxidative phosphorylation can affect BAT thermogenic activity (Kajimura & Saito, 2014). During BAT-mediated thermogenesis, UCP1 uncouples heat production from ATP synthase, therefore it is likely that defects in oxidative phosphorylation could affect this output. As mentioned above, titin can potentially modulate mitochondrial bioenergetics and transcription of oxidative phosphorylation components, and therefore could be a potential explanation for the reduced nonshivering thermogenesis capacity of *mdm* mice. Taylor-Burt et al. (2015) demonstrated a direct effect of titin stiffness on the rate of shivering. My results indicate that a nonshivering thermogenesis deficiency could reflect a regulatory effect of titin on metabolic processes. Whether these effects are due to titin signaling or other pathways is a question that could be explored in future work.

4.4 Thermogenic Capacity and its Components

Thermogenic capacity is significantly reduced in *mdm* mice compared to expected values for their body size (Taylor-Burt et al., 2015). VO_{2sum} measured in wild type and *mdm* mice was

11.1 ml O_2 $g^{-1}h^{-1}$ and 10.4 ml O_2 g^{-1} h^{-1} in comparison to predicted values of 10.5 ± 0.2 ml O_2 $g^{-1}h^{-1}$ and 14.9 ± 0.2 ml O_2 $g^{-1}h^{-1}$ (Taylor-Burt et al., 2015; Bozinovic & Rosenmann, 1989). Additionally, relative contributions of BMR, ST, and NST were not different between *mdm* and wild type mice.

Many small mammals, including deer mice, have been shown to increase their thermogenic capacity solely by altering NST after cold acclimation (Van Sant & Hammond, 2008). While NST is regarded as the most plastic component of VO_{2sum}, studies have shown that animals can increase their capacity for ST in addition to NST after cold acclimation (Nespolo, et al., 1999). One might hypothesize that animals with a deficiency in ST would increase their capacity for NST to offset the imbalance in heat generation. Therefore, these results are interesting in that *mdm* mice have a reduced thermogenic capacity for both ST and NST. Future work should investigate whether the capacity for NST can be increased in *mdm* through cold acclimation, albeit at much higher T_a's than usually used in acclimation studies such as 27-30°C, where *mdm* mice were sufficiently cold stressed (**Figure 3**).

My results show significant differences in metabolic rates as well as the capacity for nonshivering thermogenesis even before accounting for wild type mice having body masses approximately 4-fold higher than *mdm* mice. Metabolic rate and the capacity for nonshivering thermogenesis scale allometrically with body size, as mentioned previously (Kleiber, 1932) and these comparisons allowed me determine that the severe defects in thermoregulation are not just due to body size. Comparisons between *mdm* mice and the little pocket mouse demonstrated that *mdm* mice do not adapt to their small body size, as shown by their smaller metabolic rates, even at thermoneutrality (Chew et al., 1967). Additionally, as animals get smaller, their contribution of NST to thermogenic capacity increases to offset the balance in increased thermal conductance

due to increased surface area (Wunder & Gettinger, 1996). VO_2 responses to NE in *mdm* mice were almost half the size (6.4 ml O_2 g^{-1} h^{-1}) compared to predicted values (11 ml O_2 g^{-1} h^{-1}; Wunder & Gettinger, 1996). My findings demonstrate that *mdm* mice do not adapt to their small size like other small animals and that their thermoregulatory defects are either due to direct or indirect effects of the N2A deletion in titin.

I conclude that the observed hypothermia in *mdm* mice is due to contributions of multiple aspects of thermoregulation: thermal conductance, ST, and NST. Investigations of thermal conductance and thermogenic capacity provide a complete assessment of an animal's ability to thermoregulate during cold temperatures in terms of heat loss (thermal conductance) and heat production (BMR, ST, and NST). Taylor-Burt et al. (2015) found that *mdm* mice do not fail to thermoregulate solely due to small body size, which increases surface area for thermal conductance. Comparisons of *mdm* mice to size-matched *Baiomys taylori* showed significant differences in thermal conductance, suggesting that increased thermal conductance is due to other factors such as low levels of insulating white adipose tissue or perhaps fur quality. My results demonstrate that the rate of heat loss exceeds the rate of heat production in *mdm* mice, as demonstrated by impairments in both ST (Taylor-Burt et al., 2015) and NST in addition to increased thermal conductance.

4.5 Conclusions

The results of this study demonstrate that not only does a deletion in N2A titin affect the rate of shivering in *mdm* mice, but it also reduces thermogenic capacity and nonshivering thermogenesis. This mutation severely affects the thermoregulatory abilities of *mdm* mice so that *mdm* mice cannot maintain normal T_b's below 34°C due to deficiencies in shivering

thermogenesis, nonshivering thermogenesis, and increased thermal conductance. When comparisons are made to account for the small body size of *mdm* mice, these deficiencies are exacerbated. It is not clear how titin could modulate nonshivering thermogenesis, but it could be through an indirect role in regulating oxidative phosphorylation or other pathways. Future studies should investigate these possible links.

References

Bal, N. C., Maurya, S. K., Sopariwala, D. H., Sahoo, S. K., Gupta, S. C., Shaikh, S. A., … Periasamy, M. (2012). Sarcolipin is a newly identified regulator of muscle-based thermogenesis in mammals. *Nature Medicine*, *18*(10), 1575–1579. https://doi.org/10.1038/nm.2897

Bowman, W. C. (2006). Neuromuscular block. *British Journal of Pharmacology*, *147*(SUPPL. 1), 277–286. https://doi.org/10.1038/sj.bjp.0706404

Bozinovic, F., & Rosenmann, M. (1989). Maximum metabolic rate of rodents: physiological and ecological consequences on distributional limits. *Functional Ecology*, *3*(2), 173–181. https://doi.org/10.2307/2389298

Cannon, B; Nedergaard, J. (2004). Brown Adipose Tissue : Function and Physiological Significance. *Physiological Reviews*, *84*(1), 277–359.

Chew, R. M., Lindberg, R. G., & Hayden, P. (1967). Temperature regulation in the little pocket mouse, Perognathus longimembris. *Comparative Biochemistry And Physiology*, *21*(3), 487–505. https://doi.org/10.1016/0010-406X(67)90447-1

Depocas, F. (1960). The calorigenic response of cold-acclimated white rats to infused noradrenaline. *Biochemistry and Cell Biology*, *38*(2), 107–114. https://doi.org/10.1139/o60-012

Garvey, S. M., Rajan, C., Lerner, A. P., Frankel, W. N., & Cox, G. A. (2002). The muscular dystrophy with myositis (mdm) mouse mutation disrupts a skeletal muscle-specific domain of titin. *Genomics*. https://doi.org/10.1006/geno.2002.6685

Geiser, F., Currie, S. E., O'Shea, K. A., & Hiebert, S. M. (2014). Torpor and hypothermia: reversed hysteresis of metabolic rate and body temperature. *AJP: Regulatory, Integrative and Comparative Physiology*, *307*(11), R1324–R1329. https://doi.org/10.1152/ajpregu.00214.2014

Golozoubova, V. (2006). UCP1 is essential for adaptive adrenergic nonshivering thermogenesis. *AJP: Endocrinology and Metabolism*, *291*(2), E350–E357. https://doi.org/10.1152/ajpendo.00387.2005

Guerra, C., Koza, R. A., Walsh, K., Kurtz, D. M., Wood, P. A., & Kozak, L. P. (1998). Abnormal nonshivering thermogenesis in mice with inherited defects of fatty acid oxidation. *Journal of Clinical Investigation*, *102*(9), 1724–1731. https://doi.org/10.1172/JCI4532

Hemingway, A. (1963). Shivering. *Physiological Reviews*.

Hessel, A. L., Lindstedt, S. L., & Nishikawa, K. C. (2017). Physiological Mechanisms of Eccentric Contraction and Its Applications: A Role for the Giant Titin Protein. *Frontiers in Physiology*, *8*. https://doi.org/10.3389/fphys.2017.00070

Hudson, J. W., & Scott, I. M. (1978). Daily Torpor in the Laboratory Mouse , Mus musculus Var . Albino. *Physiological Zoology*, *52*(2), 205–218.

Huebsch, K. A., Kudryashova, E., Wooley, C. M., Sher, R. B., Seburn, K. L., Spencer, M. J., & Cox, G. A. (2005). Mdm muscular dystrophy: Interactions with calpain 3 and a novel functional role for titin's N2A domain. *Human Molecular Genetics*, *14*(19), 2801–2811. https://doi.org/10.1093/hmg/ddi313

Jumbo-Lucioni, P., Bu, S., Harbison, S. T., Slaughter, J. C., Mackay, T. F. C., Moellering, D. R., & De Luca, M. (2012). Nuclear genomic control of naturally occurring variation in mitochondrial function in Drosophila melanogaster. *BMC Genomics*, *13*(1). https://doi.org/10.1186/1471-2164-13-659

Kajimura, S., & Saito, M. (2014). A New Era in Brown Adipose Tissue Biology: Molecular Control of Brown Fat Development and Energy Homeostasis Shingo. *Annu Rev Physiol.*, (1), 225–249. https://doi.org/10.1146/annurev-physiol-021113-170252.A

Kashimura, O., Sakai, A., Yanagidaira, Y., & Ueda, G. (1992). Thermogenesis Induced by Inhibition of Shivering During Cold Exposure in Exercise-Trained Rats. *Aviation Space and Environmental Medicine*, *63*(12), 1082–1086.

Kleiber, M. (1932). Body Size and Metabolism. *California Agricultural Experiment Station*, *6*(11), 315–353. Retrieved from http://hilgardia.ucanr.edu/fileaccess.cfm?article=152052&p=VOWQRB

Lopez, M. A., Pardo, P. S., Cox, G. A., & Boriek, A. M. (2008). Early mechanical dysfunction of the diaphragm in the muscular dystrophy with myositis (Ttnmdm) model. *AJP: Cell Physiology*, *295*(5), C1092–C1102. https://doi.org/10.1152/ajpcell.16.2008

Lowell, B., S-Susulic, V., Hamann, A., Lawitts, J., Himms-Hagen, J., Boyer, B., … Flier, J. (1993). Development of obesity in transgenic mice after genetic ablation of brown adipose tissue. *Nature*, *366*, 740–742. Retrieved from http://dx.doi.org/10.1038/366740a0

Madden, C. J., & Morrison, S. F. (2016). A high-fat diet impairs cooling-evoked brown adipose tissue activation via a vagal afferent mechanism. *American Journal of Physiology - Endocrinology And Metabolism*, *311*(2), E287–E292. https://doi.org/10.1152/ajpendo.00081.2016

Meyer, C. W., Willershäuser, M., Jastroch, M., Rourke, B. C., Fromme, T., Oelkrug, R., … Klingenspor, M. (2010). Adaptive thermogenesis and thermal conductance in wild-type and UCP1-KO mice. *American Journal of Physiology - Regulatory, Integrative and Comparative Physiology*, *299*(5). Retrieved from http://ajpregu.physiology.org/content/299/5/R1396.long

Morrison, S. F., & Nakamura, K. (2011). Central neural pathways for thermoregulation. *Frontiers in Bioscience (Landmark Edition)*, *16*, 74–104. https://doi.org/10.2741/3677

Nedergaard, J., Golozoubova, V., Matthias, A., Asadi, A., Jacobsson, A., & Cannon, B. (2001). UCP1: The only protein able to mediate adaptive non-shivering thermogenesis and metabolic inefficiency. *Biochimica et Biophysica Acta - Bioenergetics*, *1504*(1), 82–106. https://doi.org/10.1016/S0005-2728(00)00247-4

Nespolo, R. F., Opazo, J. C., Rosenmann, M., & Bozinovic, F. (1999). Thermal acclimation, maximum metabolic rate, and nonshivering thermogenesis of Phyllotis xanthopygus (rodentia) in the Andes mountains. *Journal of Mammalogy*, *80*(3), 742–748. https://doi.org/10.2307/1383243

Nicholls, G., & Locke, R. (1984). Thermogenic Mechanisms in Brown Fat. *The American Physiological Society*, *64*(1), 1–64.

Pace, C. M., Mortimer, S., Monroy, J. A., & Nishikawa, K. C. (2017). The effects of a skeletal muscle titin mutation on walking in mice. *Journal of Comparative Physiology A*, *203*(1), 67–76. https://doi.org/10.1007/s00359-016-1137-5

Rowland, L., Bal, N., & Periasamy, M. (2015). The role of skeletal-muscle-based thermogenic mechanisms in vertebrate endothermy. *Biol Rev Camb Philos Soc.*, *90*(4), 1279–1297. https://doi.org/10.1126/science.1249098.Sleep

Sakaguchi, T., Arase, K., Fisler, J. S., & Bray, G. A. (1989). Effect of a high-fat diet on firing rate of sympathetic nerves innervating brown adipose tissue in anesthetized rats. *Physiology and Behavior*, *45*(6), 1177–1182. https://doi.org/10.1016/0031-9384(89)90106-6

Speakman, J. R. (2013). Measuring energy metabolism in the mouse - theoretical, practical, and

analytical considerations. *Frontiers in Physiology*, *4 MAR*(March 2013). https://doi.org/10.3389/fphys.2013.00034

Taylor-Burt, K. R., Monroy, J., Pace, C., Lindstedt, S., & Nishikawa, K. C. (2015). Shiver me titin! Elucidating titin's role in shivering thermogenesis. *Journal of Experimental Biology*, *218*(5), 694–702. https://doi.org/10.1242/jeb.111849

Townsend, K., & Tseng, Y.-H. (2014). Brown Fat Fuel Utilization and Thermogenesis. *Trends Endocrinol Metab*, *25*(4), 168–177. https://doi.org/10.3174/ajnr.A1256.Functional

Van Sant, M. J., & Hammond, K. A. (2008). Contribution of Shivering and Nonshivering Thermogenesis to Thermogenic Capacity for the Deer Mouse (Peromyscus maniculatus). *Physiological and Biochemical Zoology*, *81*(5), 605–611.

Verdonschot, J. A. J., Hazebroek, M. R., Derks, K. W. J., Barandiarán Aizpurua, A., Merken, J. J., Wang, P., … Heymans, S. R. B. (2018). Titin cardiomyopathy leads to altered mitochondrial energetics, increased fibrosis and long-term life-threatening arrhythmias. *European Heart Journal*, (February), 1–10. https://doi.org/10.1093/eurheartj/ehx808

Wunder, B. A., & Gettinger, R. D. (1996). Effects of body mass and temperature acclimation on the nonshivering thermogenic response of small mammals. *Adaptations to the Cold: Tenth International Hibernation Symposium*.

Yen, T. T., Fuller, R. W., & Pearson, D. V. (1974). The response of "obese" (ob/ob) and "diabetic" (db/db) mice to treatments that influence body temperature. *Comparative Biochemistry and Physiology -- Part A: Physiology*, *49*(2), 377–385. https://doi.org/10.1016/0300-9629(74)90128-5